MNRAS 000, 1–7 (2022) Preprint 27 April 2022 Compiled using MNRAS LATEX style file v3.0

Impact of core-collapse supernova models on the population of binary black holes

Francesco Iraci[1]⋆
[1] *Physics and Astronomy Department Galileo Galilei, University of Padova, Vicolo dell'Osservatorio 3, I–35122, Padova, Italy*

27 April 2022

ABSTRACT

I investigate the impact of different core-collapse supernova (CCSN) models on the population of binary black holes (BBHs) using the population synthesis code `SEVN`. I generate a set of 10^4 binary systems with fixed metallicity $Z = 0.002$ and mass range for primary stars $[5, 150]\,M_\odot$ and I study the BHs mass spectrum using three different CCSN prescriptions: Rapid, Delayed, Compactness. For the last model I choose three different the compactness parameter: $\xi_{2.5}$ taken from Patton & Sukhbold (2020) distribution; $\xi_{2.5} = 0.2$; $\xi_{2.5} = 0.4$. I will show the relation between remnants and initial stars mass and I'll focus on the mass gap Neutron stars-Black holes.

Key words: astrophysical black holes – supernovae: general – stars: binaries – binary black holes

1 INTRODUCTION

Understanding the final fate of a massive stare is essential in order to estimate some of the outcomes of its explosion. These include the goal of explaining the black holes (BHs) mass function, which is still an open question in modern astrophysics.

Stars with zero-age main sequence mass range $8M_\odot \lesssim M_{\rm ZAMS} \lesssim 150M_\odot$ end their lives with the gravitationally induced catastrophic collapse of their electron-degenerate iron core to nuclear densities. The supernova explosion mechanism, the so called core-collapse supernova (CCSN) (JANKA et al. (2007)), is triggered when the mass of the central degenerate core reaches the Chandrasekar limit (Chandrasekhar (1931)). Thus, when the iron core reaches about $1.44M_\odot$, electron degeneracy pressure can no longer stabilize the core and it collapses. Due to electron capture, lots of neutrinos (ν_e) are produced and when the density reaches $\rho_{\rm trap} \simeq 10^{12}\,{\rm g/cm^3}$ there's an important change in the physics of the collapse: neutrinos are trapped in the core because their diffusion time becomes longer than the time of collapse, so it continues until the density reaches $\rho \approx 10^{14}{\rm g/cm^3}$. Neutrons become degenerate and the equation of state (EoS) becomes stiff. Nuclear matter has much lower compressibility, so the core decelerates and bounces in response to the increased nuclear matter pressure. The shock initially races through the still collapsing outer core, but soon stalls and turns into an accretion shock due to the dissociation of heavy nuclei at the shock front and neutrino losses from the post-shock region (Bethe (1990)). The stalled shock can be revived by neutrinos streaming off the neutrinosphere (delayed-neutrino mechanism). The energy input given by neutrinos drives the shock outwards again, eventually leading to supernova (SN) explosion. Whether a star explodes or not depends on its properties at the onset of collapse. If mass and central compactness are sufficiently high a star may even avoid explosion, collapsing quietly to a BH, producing a more massive remnant than in the case of a supernova explosion. It's therefore crucial to accurately describe the final stage of a star's life.

In this paper I consider an initial population of 10^4 isolated binary systems. Binary population-synthesis codes have been used to investigate the effect of binary evolution processes on the formation of BBHs in isolated binaries. In these semi-analytic codes there is a combined description of stellar evolution with prescriptions for SN explosions and with a formalism for binary evolution processes. An isolated binary system is composed by two gravitationally bounded stars. Initially both of them are on the main sequence (MS). When the most massive one leaves MS its radius grows and equals the Roche lobe which is a drop-shaped equipotential surface that surrounds the star. The Roche lobes of two objects in a binary are connected in just one point (Lagrangian point) through which mass transfers from a star (the primary) to the lighter one (the secondary). After several evolutionary stages the primary collapses quietly to a BH. This happens if I want a remnant to be $> 20M_\odot$ and if I want the binary to remain bound. Direct collapse indeed implies almost no kick, while SN explosion could unbound the system. Then, when the secondary leaves the MS, growing in radius the system enters in common envelope (CE) phase. If the envelope is not ejected, BH merges with the Helium core leaving a single BH. If the envelope is ejected the system remains with BH bounded with a Helium naked star. The secondary star undergoes a SN explosion or a direct collpase to a BH. If the binary system remains bound it evolves to a BBH which could merge within a Hubble time. A schematic summary of binary evolution is well illustrated in Mapelli (2021, figure 1.5).

⋆ E-mail: fracnesco.iraci.1@studenti.unipd.it

Phase int	Phase string	Physics
0	PreMainSequence	
1	MainSequence	Core H-burning start
2	TerminalMainSequence	Creation of a He core
3	HshellBurning	He core almost formed
4	HecoreBurning	Core He-burning start
5	TerminalHecoreBurning	Creation of a CO core
6	HeshellBurning	CO core almost formed
7	Remnant	Star is dead

Table 1. List of integer values used for stellar evolution phases.

RemType int	RemType string	Physics
0	NotARemnant	Star is not a remnant
1	HeWD	Helium White-Dwarf
2	COWD	CO White-Dwarf
3	ONeWD	Oxygen-Neon White-Dwarf
4	NS_{ECSN}	NS after ElectroCapture SN
5	NS_{CCSN}	NS after Core Collapse SN
6	BH	Black Hole
-1	Empty	Massless remnant

Table 2. List of integer values used for remnant types.

In this work has been used the population synthesis code `SEVN` (Mapelli et al. (2020); Spera et al. (2019)) which is able to describe single and binary stars evolution with different prescriptions for CCSN.

2 METHODS

2.1 SEVN

`SEVN` is a population synthesis code which describes stellar evolution through a set of look-up tables. These tables contain information on star mass, star radius and core radius, stellar metallicity and evolutionary stages. In this work I use a set of look-up tables generated with the code `PARSEC` (Bressan et al. (2012)). This set of tables ranges from metallicity $Z = 10^{-4} \div 4 \cdot 10^{-2}$ and stars in the mass range $2.2M_{\odot} \leq M_{ZAMS} \leq 600M_{\odot}$. In addition I have used a set of tracks for bare Helium cores (Spera et al. (2019)) to describe the evolution of stars which lose their whole Hydrogen envelop after mass transfer phase. For these tables the metallicity and mass ranges are: $Z = 10^{-4} \div 5 \cdot 10^{-2}$, $0.36M_{\odot} \leq M_{He-ZAMS} \leq 350M_{\odot}$. To perform the interpolation, in `SEVN` the lifetime of a star is divided into different stellar phases as shown in Table 1 and the remnant type is classified as shown in Table 2. In this paper I focus on population of black holes (remnant type 6).

2.2 CCSN models

`SEVN` includes different models to describe the outcome of CCSN event. In this work I have compared three of them: Rapid, Delayed and Compactness model.

2.2.1 Rapid Model

The Rapid model is described by Fryer et al. (2012) which assumes that the explosion occurs < 250 ms after the bounce. In particular it's necessary to know the mass of the star and of the CO core at the time of core-collapse. The mass of the remnant is influenced by the amount of fallback, which varies depending on the mass above the proto-compact object and the strength of the explosion. In particular the final remnant (baryonic) mass is calculated as:

$$M_{\rm rem} = M_{\rm proto} + M_{\rm fb} \tag{1}$$

where $M_{\rm proto}$ is set to 1 $M_{\odot}$. $M_{\rm fb}$ is the fallback mass and it's defined as:

$$M_{\rm fb} = f_{\rm fb}\,(M - M_{\rm proto}) \tag{2}$$

with $f_{\rm fb}$ being the fractional fallback parameter defined in Fryer et al. (2012, equation 16).

2.2.2 Delayed Model

The explosion occurs on a much longer time scale ($\gg 250$ ms) and the energy of the explosion is lower. The equation needed to calculate the remnant mass are the same of the previous model: (1) and (2), but the fractional fallback parameter changes (Fryer et al. (2012, equation 19)). The delayed explosion mechanism occurs over a longer timescale because it tends to be weaker than the rapid, producing many more explosions with energies below 10^{51} erg. The consequence is a continuous remnant mass spectrum, without the typical mass gap between NSs and BHs that is present in the Rapid model (see 3.1.1).

2.2.3 Compactness Model

The compactness of a star at the pre-supernova stage is a fundamental property that influences the core collapse and the following explosion. It is defined as (O'Connor & Ott (2011)):

$$\xi_M = \left.\frac{M/M_{\odot}}{R(M_{\rm bary} = M)/1000\ {\rm km}}\right|_{t=t_{\rm bounce}} \tag{3}$$

with $M = 2.5\,M_{\odot}$ and R being the radial coordinate that encloses a mass equal to M at the time of core bounce. In this model the parameter $\xi_{2.5}$ defines a threshold to determine whether a star becomes a BH or not. Lots of studies have been done on this parameter trying to understand which is the better choice for it. For example O'Connor & Ott (2011) suggested that progenitors with $\xi_{2.5} > 0.45$ most likely form BHs, while Horiuchi et al. (2014) used $\xi_{2.5} > 0.2$ and Mapelli et al. (2020) adopted $\xi_{2.5} > 0.3$. Here I compare the BH mass spectrum obtained from three different choices of compactness: (1) following the distribution showed in Patton & Sukhbold (2020, figure 3), at each value of the compactness parameter is associated a probability of explosion/implosion. If $\xi_{2.5} < 0.1$ no implosion occurs, if $\xi_{2.5} > 0.3$ no explosion occurs; (2) $\xi_{2.5} = 0.2$; (3) $\xi_{2.5} = 0.4$.

2.3 Initial conditions

In order to run `SEVN`'s simulations for binary and single stellar evolution it's necessary to create initial conditions. For binary

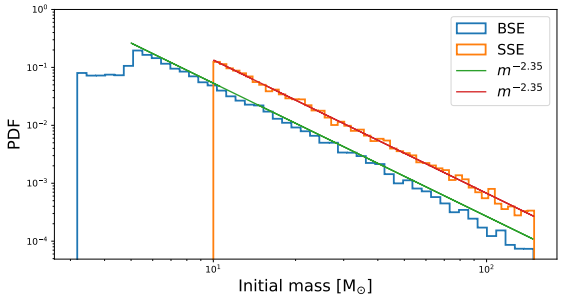

Figure 1. Initial mass function for binary stellar evolution (blue) and single stellar evolution (orange). Red line is the theoretical Kroupa mass function in the range [10,150]M$_\odot$. Green line is the theoretical Kroupa mass function in the range [5,150]M$_\odot$. Below 5 M$_\odot$ there are only secondary stars.

stellar evolution (BSE) I have generated a set of 10^4 binary stars following a Kroupa initial mass function (IMF)(Kroupa (2001)). In particular primary stars (the more massive ones) have been generated in the mass range $[5, 150]$M$_\odot$, so their IMF goes like $m^{-2.35}$, while the secondary are obtained multiplying the mass of the primary by a quantity $q < 1$, $M_2 = q\,M_1$, nearly flat distributed ($\propto q^{-0.1}$). In addition, spin has been set to zero and metallicity $Z = 0.002$. To build the IMF I didn't consider the whole domain in which the Kroupa mass function is defined. It is in fact a double power law

$$p(m) = k\,m^{-\alpha} \tag{4}$$

$$\alpha = 1.35 \text{ for } m < 0.8 \tag{5}$$

$$\alpha = 2.35 \text{ for } m > 0.8 \tag{6}$$

where k is the normalization constant. I set the lower mass limit to 0.1 M$_\odot$ so in the IMF is missing the range $[0.1, 5]\,M_\odot$. This means that I need to correct the population of BHs by a factor of 0.285 which is obtained with a proportion between the part of Kroupa I use and the one I neglect. I could have also generated stars in a range $[0.1, 150]$M$_\odot$, but `SEVN` can just evolve stars with a mass ≥ 2.2M$_\odot$ (2.1) and I would have obtained a not statistically relevant number of BHs.

Also for SSE I have generated 10^4 stars with IMF in the range $[10, 150]$M$_\odot$ (Figure 1), zero spin and metallicity $Z = 0.002$. Here it's not necessary to introduce the correction factor because I'm just interested in comparing and overlapping this simulation with the previous ones.

3 RESULTS

3.1 Impact of CCSN model on BH masses

Figure 5 shows the mass function of black holes and their relation with the zams mass for three different CCSN models. I classify in three different categories the population of BBHs: the first includes all the BBHs systems; the second consists in all BBHs systems which are bounded, so with a non-zero semimajor axis; The third includes all BBHs systems which are going to merge within a Hubble time (14 Gyrs).

From the right column of figure 5 it's possible to obtain some information on the models. The SSE track shows that some of the BHs obtained from BSE have evolved in the same way they would have done if they were without a companion. In fact, it happens that two massive stars in a binary system (eventually) become a BBH and the mass of each BH is the same as if its progenitor star was a single star if the binary system is sufficiently wide (detached binary) for its entire evolution. In all models the SSE track deviates from the bisector at $M_{\rm zams} > 30$ M$_\odot$ because of stellar winds and enters in the Pulsational Pair-Instability Supernova regime at ~ 80 M$_\odot$. This happens when the Helium-core mass is in the range $64 > m_{\rm He}/{\rm M}_\odot \geq 32$ (Mapelli et al. (2020)). Another evident feature of these plots is in the distribution of the remnants. Rapid and delayed share the same minimum zams limit ~ 12 M$_\odot$ and so do the first two compactness models at ~ 9 M$_\odot$. The last compactness model with $\xi_{2.5} = 0.4$ clearly has a greater limit. This is due to the high value of the compactness parameters, which selects more massive stars ($M_{{\rm zams}_{min}} \sim 15$ M$_\odot$). In all models the lower envelope of the plot is due to those stars that during binary evolution lost all their envelope remaining just with naked helium core and subsequently collapsing to a BH.

The mass spectra (left column Figure 5) present a multi-peak structure (Abbott et al. (2021b)). The first and most dense peak is around 10 M$_\odot$ except for the delayed model which has it at slightly lower masses. The second one for all models is ~ 15 M$_\odot$ and then there is a third peak at 30 M$_\odot$. Similar structures have been found in most recent work of the collaboration LIGO, VIRGO, KAGRA, (Abbott et al. (2021a, figure 11)) on populations of compact binaries. The fraction of merging systems is nearly ten times lower than the bounded ones (see table 3). The most critical quantities which determine whether a binary merges or not are the masses of the two stars and their initial orbital separation (with respect to the stellar radii). A BBH system usually merges within a Hubble time only if its initial orbital separation is of few tens of solar radii, but massive stars (> 20 M$_\odot$) can reach a radius of several thousands of solar radii during their evolution. Therefore, if the initial orbital separation is tens of solar radii, the binary merges before it can become a BBH. On the other hand if the initial orbital separation is too large the BHs will never merge. Thus, in order to have a merging system, the initial orbital separation of the progenitor stars must be in the range which allows the binary to enter in a CE phase and then leave a short period of BBH where gravitational waves emission leads to coalescence.

3.1.1 Rapid-Delayed

While minimum ZAMS mass is almost the same, the main difference between rapid and delayed SN model is the number of remnants in the gap $2 < M_{rem} < 5 M_\odot$. In fact the rapid model predicts a mass gap between the lightest BH (5.7 M$_\odot$) and the heaviest NS (2 M$_\odot$), while in the delayed model there's no gap and the crossing point from NS to BH is at ~ 3 M$_\odot$. This situation is very clear in figure 2 where is shown the comparison between the BH mass spectra of the two models. Rapid model has a higher peak at ~ 10 M$_\odot$, but the total number of BHs produced with the delayed model is higher due to the presence of BHs in the rapid mass gap $[3, 5]$M$_\odot$ (see table 3). The distribution for $M_{\rm BH} > 10$ M$_\odot$ is nearly the same for both models. Merging systems are as expected a small fraction of the total BHs produced, but it's

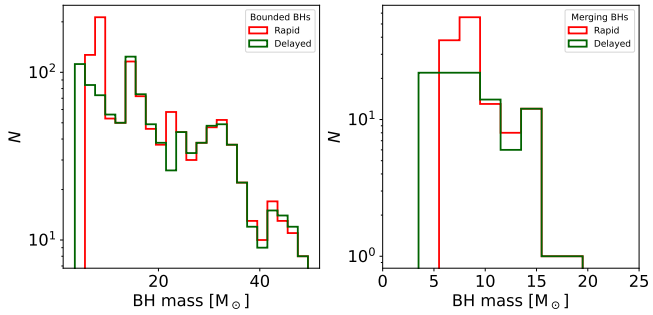

Figure 2. Comparison between Rapid (Red) and Delayed (Green) BHs populations. Left panel: Bounded systems. Right panel: Merging systems

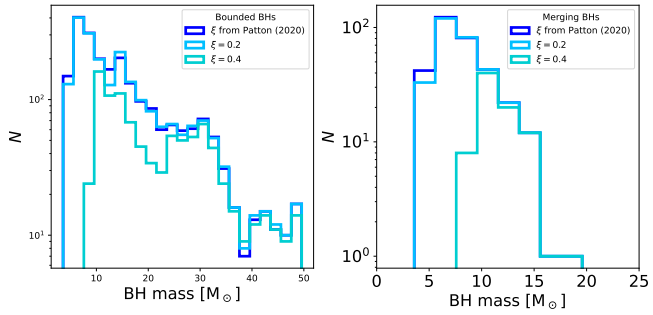

Figure 3. Comparison between the number of BHs produced changing the parameter $\xi_{2.5}$ of the Compactness model. Left panel: Bounded systems. Right panel: Merging systems.

still visible the difference in the lower mass limit between the models.

3.1.2 Compactness

In Figure 3 is shown how the BH population varies changing the value of the compactness parameter (3). Dark and light blue distributions are almost equal. In fact, using Patton & Sukhbold (2020) distribution for the parameter $\xi_{2.5}$, at each compactness value `SEVN` associates a probability $\mathcal{P}$ of explosion. If $\xi > 0.3$, $\mathcal{P} = 0$ and only implosions occurs. If $\xi < 0.1$, $\mathcal{P} = 1$ and only explosions occurs. Between these ξ values $\mathcal{P} < 1$. $\xi_{2.5} \sim 0.18$ is the crossing point of the distribution separating most of the explosions form most of the implosions. I chose the value $\xi_{2.5} = 0.2$ which is close to the crossing point and below which it's more probable to have an explosion. Therefore both compactness parameter choices give almost the same BH mass spectrum. Instead, increasing the compactness threshold ($\xi_{2.5} = 0.4$) has some consequences on the final remnant population: higher initial mass is required to reach such value of compactness indeed the minimum ZAMS mass increases ($\sim 15\,M_\odot$) and so does the minimum BH mass ($\sim 7.5\,M_\odot$). Moreover, the fraction of produced BHs decreases in the initial part of the spectrum ($< 25\,M_\odot$). The result is reasonable, in fact if I fix the mass, an increase in the compactness parameter leads to a decrease in the BHs production. Above $\sim 30\,M_\odot$ the distribution for all the three prescriptions is nearly the same. The merging spectra have, as expected, a lower number of BHs. The first two of them have a peak around $7\,M_\odot$, while for $\xi_{2.5} = 0.4$ the distribution is shifted with a peak at $\sim 11 M_\odot$.

In Figure 4 is shown the mass spectrum of all the three models together. The first thing to notice, looking at the top row, is that the number of BHs produced with the first two compactness models is higher than Rapid and Delayed model. Furthermore, the first two compactness prescriptions, similarly to delayed model, reduces the mass gap between the heaviest NS ($3\,M_\odot$) and the lightest BH ($\sim 3.5\,M_\odot$ with Patton & Sukhbold (2020), $\sim 4.4\,M_\odot$ with $\xi_{2.5} = 0.2$). $\xi_{2.5} = 0.4$ shifts the spectrum and the minimum mass to higher values and has a lower number of BHs produced than rapid and delayed. Same considerations can be applied to the bottom row, which shows the binary systems that are going to merge within a Hubble time.

The summary of all the results and the specific values obtained with the simulations are in table 3.

4 DISCUSSION

It would be interesting to discuss these results changing some parameters. First of all the number of initial binary systems, if increased by some power of 10, may give a cleaner view of the structures behind the BHs mass spectra and on the lower mass limits. Moreover, I have studied a case with fixed metallicity $Z = 0.002$, while it could be interesting to compare how the population changes studying metal poor and metal rich stars (Spera et al. (2019)). Another interesting parameter to change would be the spin: Mapelli et al. (2020) studied how it affects the BH mass considering also different metallicities but for a set of initial single stars. Introducing spin on the generated initial stars would also be helpful to study the BH population, changing stellar tracks. In this work the look-up tables are generated from the `PARSEC` code (2.1) considering an overshooting parameter of 0.5. In Figure 6 is shown the comparison between two different tracks, one with overshooting parameter 0.4, one with 0.5. Except for a higher production of BHs in all models around $40\,M_\odot$ for the 0.4 table, the spectra looks almost the same. This is expected because I'm dealing with non rotating stars and changes in the overshooting parameter do not alter significantly the outcome. The effect of overshooting would be enhanced if I introduce spin to the stars highlighting the difference between the two tables.

5 CONCLUSIONS

Starting from an initial population of 10^4 isolated binary systems, I have investigated the impact of three different CCSN models on the remnant BHs masses and their relation with the progenitor stars mass using the population synthesis code `SEVN` (Spera et al. (2019); Mapelli et al. (2020)). Metallicity has been fixed to $Z = 0.002$ and spin is set to zero. Rapid and delayed supernova models are implemented in `SEVN` following Fryer et al. (2012). Compactness model is based on the compactness parameter defined in eq (3) (O'Connor & Ott (2011)) and I adopted three different parameter choices: $\xi_{2.5}$ following the distribution of Patton & Sukhbold (2020);

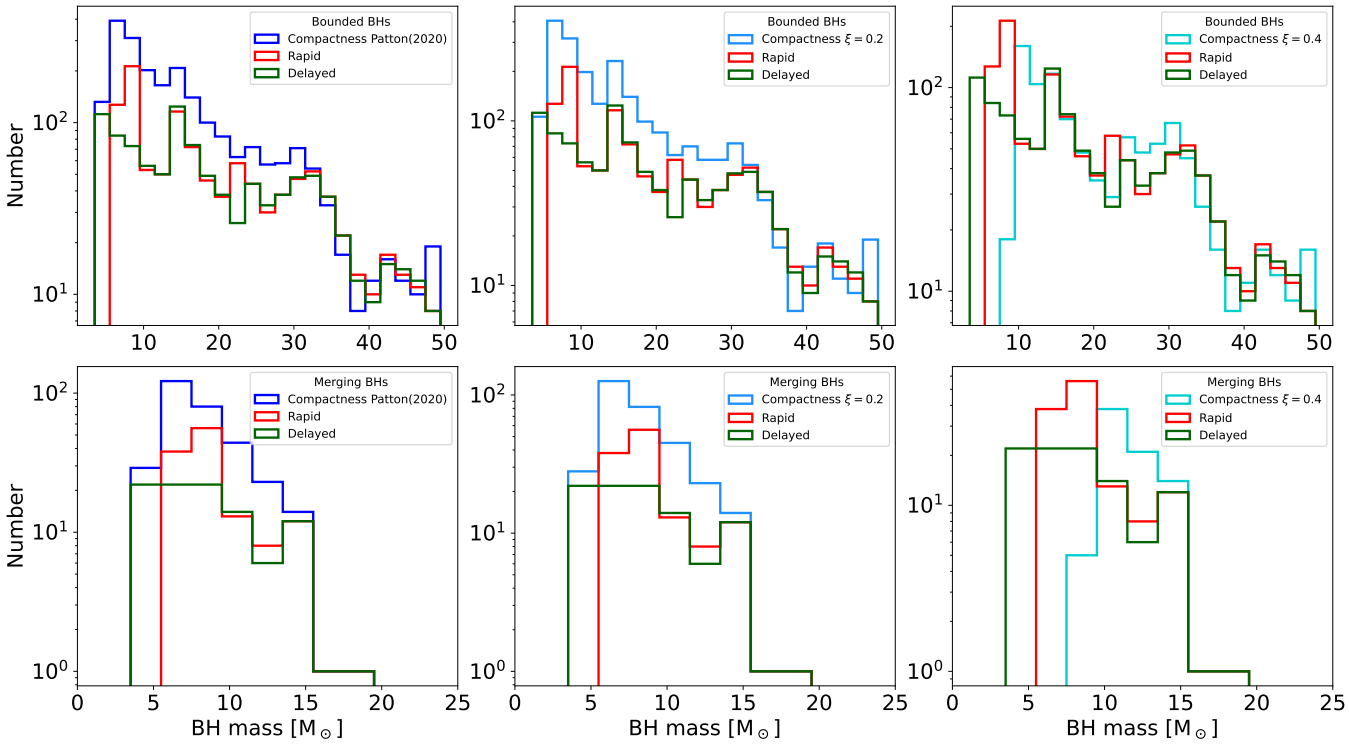

Figure 4. Comparison of the BHs mass spectrum between the three models. Top row: Bounded BBHs systems. Bottom row: Merging BBHs systems

CCSN model	Rapid	Delayed	$\xi_{2.5}$ from Patton & Sukhbold (2020)	$\xi_{2.5} = 0.2$	$\xi_{2.5} = 0.4$
All BHs produced (%)	4.16	4.64	7.31	7.17	3.50
Bounded BHs produced (%)	3.23	3.10	6.36	6.29	2.76
Merging BHs produced (%)	0.37	0.31	0.89	0.91	0.23
Minimum ZAMS mass [$M_\odot$]	12.38	12.214	9.059	9.593	15.185
Minimum BH mass [$M_\odot$]	5.701	3.001	3.498	4.429	7.685

Table 3. First three rows: percentage of BHs produced (already multiplied by the factor 0.285 (see 2.3)) starting from 10^4 binary systems. Last two rows: minimum initial mass, minimum remnant mass.

$\xi_{2.5} = 0.2$; $\xi_{2.5} = 0.4$. Rapid and delayed have almost the same minimum ZAMS mass ($\sim 12\,M_\odot$), but the first two compactness models are able to reach lower ZAMS mass values ($\sim 9\,M_\odot$). Last compactness model ($\xi_{2.5} = 0.4$) has a higher minimum ZAMS mass ($\sim 15\,M_\odot$) because of the larger compactness parameter. The fraction of BHs produced is almost the same for rapid and delayed ($4 \div 5\,\%$) and for the first two compactness models ($7 \div 8\,\%$). Again $\xi_{2.5} = 0.4$ produces less remnants because of high compactness parameter ($3.5\,\%$). Fraction of merging systems is nearly ten times lower than the total BHs produced for almost all models and the ones that produce more merging systems are the first two compactness. Small number of merging systems is expected: initial stars must be in a specific configuration which depends on masses and orbital separation. In the end I investigated how the minimum BH mass changes with the CCSN model. Rapid model present a mass gap between the heaviest NS ($2\,M_\odot$) and the lightest BH ($5.7\,M_\odot$), while delayed, because of its less constrained condition on onset of explosion, is able to completely eliminate the gap with the transition point NS-BH set at $3\,M_\odot$. Also first two compactness models diminish the gap having the lowest BH mass respectively at $3.498\,M_\odot$ and $4.429\,M_\odot$. The last compactness model has a shifted mass spectrum to higher mass values and its minimum BH mass is of $7.685\,M_\odot$.

Overall, CCSN models have a crucial impact on the mass function of BHs. Trying to understand which one better represents the data is crucial in order to interpret future gravitational waves signals coming from BBH coalescence.

REFERENCES

Abbott R., et al., 2021a
Abbott R., et al., 2021b, Astrophys. J. Lett., 913, L7
Bethe H. A., 1990, Rev. Mod. Phys., 62, 801
Bressan A., Marigo P., Girardi L., Salasnich B., Cero C. D., Rubele S., Nanni A., 2012, Monthly Notices of the Royal Astronomical Society, 427, 127

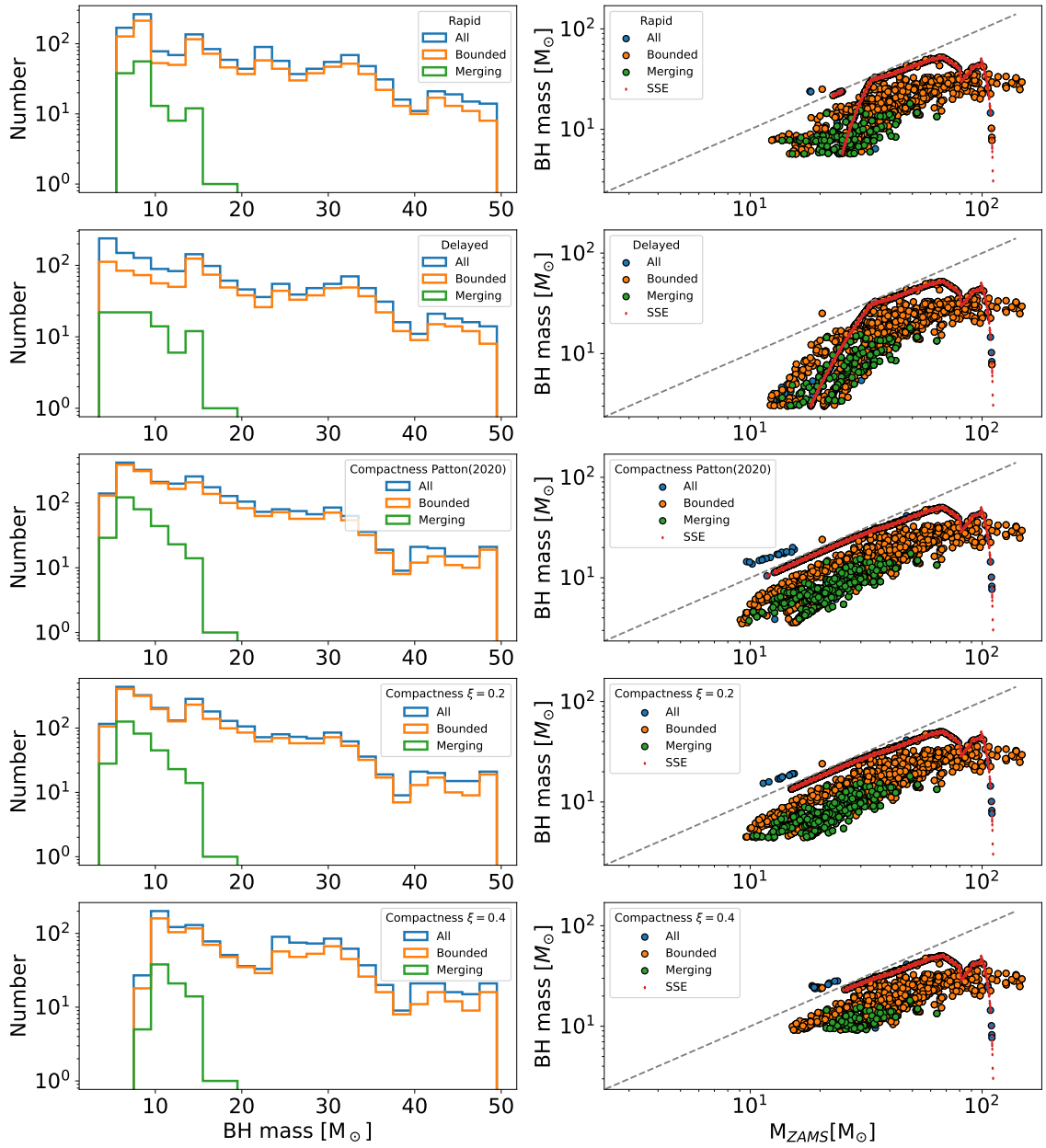

Figure 5. Left column: BHs mass spectrum. Right column: BH mass vs ZAMS mass. From top to bottom row: Rapid model; Delayed model; Compactness model with $\xi_{2.5}$ from Patton & Sukhbold (2020); Compactness model with $\xi_{2.5} = 0.2$; Compactness model with $\xi_{2.5} = 0.4$. Blue line/dots: All BBHs systems; Orange line/dots: All bounded BBHs systems; Green line/dots: All BBHs systems which are going to merge within a Hubble time (14 Gyrs). Red dots: BHs from SSE

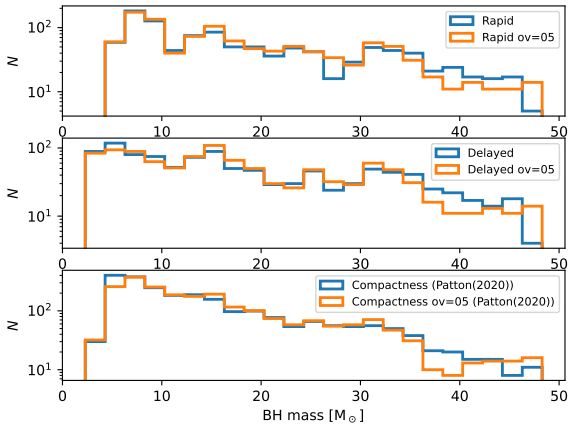

Figure 6. Comparison of BH spectra using two different tables: overshooting parameter 0.4 (Blue); overshooting parameter 0.5 (Orange). From top to bottom: Rapid model, Delayed model, Compatness Patton & Sukhbold (2020) model.

Chandrasekhar S., 1931, The Astrophysical Journal, 74, 81
Fryer C. L., Belczynski K., Wiktorowicz G., Dominik M., Kalogera V., Holz D. E., 2012, The Astrophysical Journal, 749, 91
Horiuchi S., Nakamura K., Takiwaki T., Kotake K., Tanaka M., 2014, Monthly Notices of the Royal Astronomical Society: Letters, 445, L99
JANKA H., LANGANKE K., MAREK A., MARTINEZPINEDO G., MULLER B., 2007, Physics Reports, 442, 38
Kroupa P., 2001, Monthly Notices of the Royal Astronomical Society, 322, 231
Mapelli M., 2021, in , Handbook of Gravitational Wave Astronomy. Springer Singapore, pp 1–65, doi:10.1007/978-981-15-4702-7_16-1, https://doi.org/10.1007%2F978-981-15-4702-7_16-1
Mapelli M., Spera M., Montanari E., Limongi M., Chieffi A., Giacobbo N., Bressan A., Bouffanais Y., 2020, The Astrophysical Journal, 888, 76
O'Connor E., Ott C. D., 2011, The Astrophysical Journal, 730, 70
Patton R. A., Sukhbold T., 2020, Monthly Notices of the Royal Astronomical Society, 499, 2803
Spera M., Mapelli M., Giacobbo N., Trani A. A., Bressan A., Costa G., 2019, Monthly Notices of the Royal Astronomical Society, 485, 889

This paper has been typeset from a TEX/LATEX file prepared by the author.